Original Article

A frequency domain comparison of disturbance observer based control schemes

Abdurrahman Bayrak[1,2] (iD) and Mehmet Önder Efe[3]

Abstract

In this article, an analysis and synthesis of widely used linear disturbance observer based robust control approaches are presented. The main objective of this article is to provide an exhaustive comparison of disturbance observer based robust control approaches and to handle the structural details of each approach for gaining insight about the complexity of each approach. Toward this goal, nine performances and robustness equations portraying useful insights for understanding and analyzing control systems are derived by examining their common and equivalent block diagrams. Four of them are selected as gang of four equations, namely complementary sensitivity function, sensitivity function, disturbance sensitivity function and noise sensitivity function. Robustness and disturbance rejection performance analysis of all linear disturbance observer based control schemes and classical feedback control scheme are done using gang of four equations. With these representations, two tables discussing all prime issues and facilitating the selection of the best approach are obtained. Our research stipulates critical facts and figures of each scheme by considering the derived gang of four equations, which can be used for choosing the most appropriate disturbance observer based control approach for a given robust control problem. It is concluded that the uncertainty disturbance estimator approach is superior when time delay type uncertainty is involved in the model. Unfolding this is critical as time delay is an inevitable fact in most industrial control systems. The findings also emphasize that time domain disturbance observer based control approach is proficient if there is no process time delay.

Introduction

The aim of the robust control is to deal with plant uncertainties and disturbances that widely exist in all realistic feedback systems. Since 1970s, significant number of linear and nonlinear robust control methods eliminating the adverse effects of disturbances and uncertainties has been presented in the literature. Disturbance observer based control (DOBC) is one of the most popular and powerful robust control techniques. DOBC actually is a patch over existing classical feedback controller, which has good stability and tracking performance yet it is vulnerable to external disturbances and uncertainties. The main idea of DOBC approaches is to estimate the lumped disturbances, including both unknown dynamics and external disturbances, and to achieve robustness of the overall system through cancelation/rejection/attenuation of estimated disturbances by considering a number of design issues (e.g. nominal plant, reference model, low pass filter (LPF) design, etc.) with their two degrees of freedom (2-DoF) control structures. 2-DoF control structure adds an inner loop that is activated in the presence of the uncertainties and disturbances to classical feedback

[1]Graduate School of Science and Engineering, Department of Computer Engineering, Hacettepe University, Ankara, Turkey
[2]Unmanned and Autonomous Systems, System Engineering Department, ASELSAN Inc., Ankara, Turkey
[3]Department of Computer Engineering, Hacettepe University, Ankara, Turkey

Corresponding author:
Abdurrahman Bayrak, Graduate School of Science and Engineering, Department of Computer Engineering, Hacettepe University, Beytepe Campus, Beytepe 06532, Ankara, Turkey.
Email: abayrak26@gmail.com

control (CFC) that includes a baseline controller. While the baseline controller specifies the performance and stability of the control system, the inner loop determines the disturbance rejection and uncertainty handling capabilities.[1]

The algorithm was first proposed by Ohnishi to estimate the external disturbances and structural uncertainties.[2–4] Extended state observer (ESO), so called active disturbance rejection control (ADRC) that was proposed by Han,[5,6] appears as another popular robust control scheme. Thanks to Ohnishi's and Han's inspirations to other researchers, in the last few decades, several DOBC structures are reported in the literature.[1,3,7–19]

The first general DOBC scheme, abbreviated as conventional disturbance observer based control (CDOBC), was proposed by Ohishi et al.[3] Chang et al.[7] have recommended a disturbance observer design and analysis toolbox for MATLAB to find acceptable Q-Filter for CDOBC approach. They have also studied the robust stability and nominal performance recovery analyses, which help engineers to construct CDOBC approach. A discussion on discrete implementation of CDOBC approach has been presented for motion control systems.[8] Efe and Kasnakoğlu[9] have inserted a signum function into CDOBC loop and obtained an enhanced bandwidth CDOBC scheme. A disturbance attenuation problem for a missile system using a recently proposed disturbance observer based robust control method is presented in the work of Yang et al.,[10] which is called time domain disturbance observer based control (TDDOBC). Lazim et al.[11] have applied TDDOBC approach to the formation flights of the multiple quadrotors in the presence of the external disturbances. In the study of Kürkçü et al.,[12] authors have proposed the novel DOBC method combining integral sliding mode control (ISMC) with an $\mathcal{H}_\infty$ controller named as output error-based disturbance observer based control (OEBDOBC). The works of She et al.[13,14] are the motivating studies for the equivalent input disturbance (EID) approach to improve disturbance rejection performance of control systems. An improved EID approach is presented and validated on position control of a ball-and-beam system experimentally.[15] Zhong and colleagues[16,17] have proposed uncertainty disturbance estimator (UDE) method that is an alternative control strategy to time delay control (TDC) scheme. Aharon et al.[18] have presented a guideline including the analysis of UDE approach considering actuator dynamics and applied it to power control of a multimode bidirectional non-inverting buck–boost converter. The recent and advanced DOBC approaches addressing both linear and nonlinear cases can be found in the works of Chen et al.[1] and Li et al.[19] Moreover, the reader may refer to the article of Sariyildiz et al.[20] for a detailed overview of DOBC from origin to present.

Although there are a number of DOBC schemes, robust stability and robustness performance analysis are still the problems that worth studying in this field.[19,21,22] In the studies of Sariyildiz and Ohnishi,[21,22] analysis and design of CDOBC approach is presented. However, there is not a common way to synthesize and analyze the other DOBC approaches. The only common issue known is that the designed LPF dynamics directly affects the disturbance rejection capability of the control system. Reference signal tracking capability, rejection of external disturbances, measurement noise and process variations are the basic requirements for a robust control system design. In this article, performance and robustness analysis equations of the DOBC approaches described above are derived under the presence of a number of requirements. The main contributions of this article can be summarized as follows:

- This article gives an exhaustive comparison of disturbance observer based robust control approaches. Toward this goal, nine relations between the input and the output signals, including both the baseline controller and the inner loop, are derived from the CFC for all DOBC schemes described above. Spectra of these nine transfer functions (TFs) can provide useful insights for understanding and analyzing control systems under DOBC approaches. However, in this article, the only gang of four (GoF) equations are considered, these are complementary sensitivity function (CSF), sensitivity function (SF), disturbance sensitivity function (DSF), and noise sensitivity function (NSF).
- This study stipulates the critical facts and figures of each scheme by considering the derived GoF equations, which can be used for choosing the most appropriate DOBC approach for a given robust control problem, including both minimum-phase uncertain and time-delay systems, from disturbance rejection capability to design challenges.
- In this article, the one finds the structural details of each approach and gains insight about the complexity of each approach, which is undoubtedly essential in practice. Therefore, a discussion, which is not specific to a particular plant model, is presented and a second order plant model with some uncertainty in the form of time delay is considered. Although the studied plant model is an abstract one, this makes it possible to compare the most critical aspects peculiar only to DOBC algorithms.
- After reading this work, one would have a clear understanding of which approach to choose and what to expect. From this point of view, one can extend the results seen here to a large class of dynamic systems, especially the second order ones appearing typically in mechanics.

The remaining sections of the article are organized as follows: In "Analysis and Synthesis" section, nine relations between the input and the output signals,
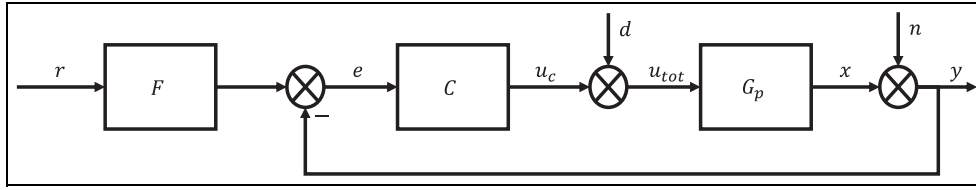
Figure 1. General block diagram of CFC.

including both baseline controller and inner loop, are derived from the CFC to five DOBC approaches described above and GoF equations are presented. "Simulation Results" section presents the operating conditions, performance and robustness analyses. The last section is devoted to the concluding remarks.

Analysis and synthesis

This section describes the derivation of the nine TFs between the input and the output signals from CFC to five DOBC approaches. Let u_c, x, y denote the controller output, the noiseless plant output and the noisy plant output, respectively. Let r, d, n denote the external influences on the closed loop systems stand for the reference signal, disturbance input and the measurement noise, respectively. We will derive the nine TFs to understand the effect of each input on each output.

CFC

Figure 1 shows CFC block diagram, including two blocks, namely, the feedback block C and the feedforward block F. In the figure, G_p is the disturbed uncertain plant. Let e denotes the reference tracking error and u_{tot} denotes the manipulated total control signal. Consider the diagram shown in Figure 1, assume that the capital letters denote the Laplace transform of the relevant variables.

From Figure 1, the following equations can be written

$$E = FR - Y \tag{1}$$

$$U_c = CE \tag{2}$$

$$U_{tot} = U_c + D \tag{3}$$

$$X = G_p U_{tot} \tag{4}$$

$$Y = X + N \tag{5}$$

The nine TFs for a CFC system can be obtained using equations (1)–(5) as follows

$$U_c = \frac{CF}{1 + G_p C} R - \frac{G_p C}{1 + G_p C} D - \frac{C}{1 + G_p C} N \tag{6}$$

$$X = \frac{G_p CF}{1 + G_p C} R + \frac{G_p}{1 + G_p C} D - \frac{G_p C}{1 + G_p C} N \tag{7}$$

$$Y = \frac{G_p CF}{1 + G_p C} R + \frac{G_p}{1 + G_p C} D + \frac{1}{1 + G_p C} N \tag{8}$$

CDOBC approach

Let d_l denotes the lumped disturbances and $\hat{d}$ denotes the estimation of lumped disturbances. Let u denotes the corrected control signal. Let G_n, G_n^{-1} and Q are the nominal model of plant, the inverse of nominal plant and disturbance observer filter, respectively. Figure 2 illustrates the original form of CDOBC.[3] Its equivalent block diagram can be obtained by replacing G_p with G_n and d with d_l. The difference between the original form and the equivalent form is that the equivalent form employs G_n as the plant, whereas the original form employs G_p, the uncertain model. As a consequence of this, $\hat{d}$ variable directly equals to lumped disturbance. However, $\hat{d}$ variable in the original form is the estimation of the lumped disturbances, obtaining which is the ultimate goal in any DOBC mechanism. Lumped disturbances include both the external disturbances and the internal disturbances caused by model uncertainties.

The following equation can be written using the noiseless plant output in Figure 2 and CDOBC equivalent block diagram

$$(U + D)G_p = (U + D_l)G_n \tag{9}$$

As a consequence, the lumped disturbances are obtained as follows

$$D_l = G_n^{-1} G_p D + (G_n^{-1} G_p - 1)U \tag{10}$$

From CDOBC equivalent block diagram, we have

$$\hat{D} = Q(D_l + G_n^{-1} N) \tag{11}$$

When we write the plant output, $X(s)$ as $X = P_n(s)U_c - Q(s)N - P_n(s)(1 - Q(s))D$ following can be said: To suppress the effects of noise, Q should go to zero. However, to avoid the adverse effects of the disturbance, Q should go to unity. These two requirements are conflicting and this fact leads to the design of
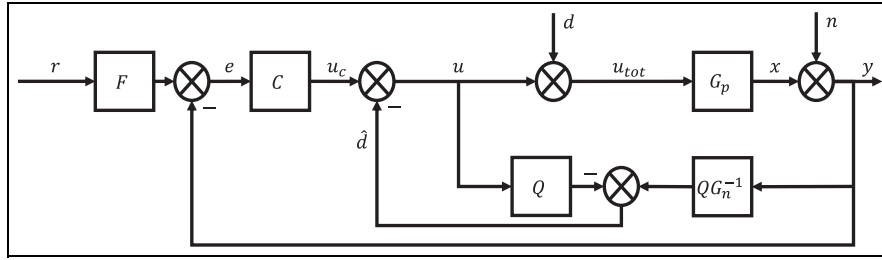
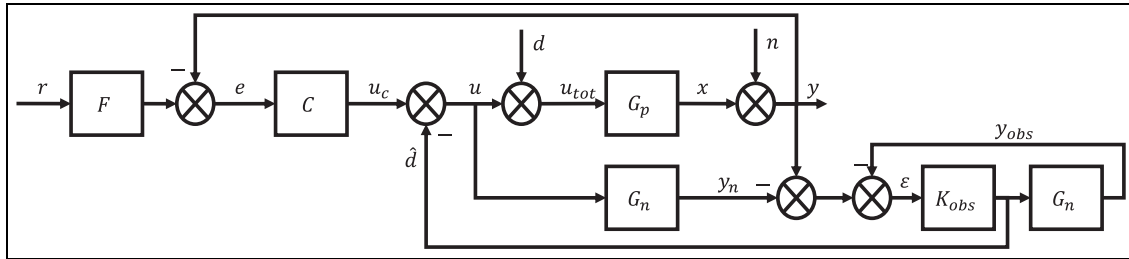**Figure 2.** General block diagram of CDOBC.

Figure 3. General block diagram of OEBDOBC.

the LPF denoted by Q. We know that disturbance ($D(s)$) has low frequency components, and noise ($N(s)$) has high frequency components; this fact entails choosing an appropriate pass band for the LPF.

From Figure 2, it can be seen that the CDOBC structure contains the CFC structure. Therefore, the first five equations in CFC section can be used with the following correction for derivation of the nine relations

$$U_{tot} = U + D \tag{12}$$

Corrected control signal U is as follows

$$U = U_c - \hat{D} \tag{13}$$

Having these in mind, the nine relations for a CDOBC system can be obtained as below. From equations (2), (10), (11) and (13), we have

$$U = \frac{CF}{1 + G_pC + Q(G_n^{-1}G_p - 1)}R$$
$$- \frac{G_p(C + QG_n^{-1})}{1 + G_pC + Q(G_n^{-1}G_p - 1)}D \tag{14}$$
$$- \frac{C + QG_n^{-1}}{1 + G_pC + Q(G_n^{-1}G_p - 1)}N$$

From equations (4), (12) and (14), we have

$$X = \frac{G_pCF}{1 + G_pC + Q(G_n^{-1}G_p - 1)}R$$
$$+ \frac{G_p(1 - Q)}{1 + G_pC + Q(G_n^{-1}G_p - 1)}D \tag{15}$$
$$- \frac{G_p(C + QG_n^{-1})}{1 + G_pC + Q(G_n^{-1}G_p - 1)}N$$

From equations (5) and (15), we have

$$Y = \frac{G_pCF}{1 + G_pC + Q(G_n^{-1}G_p - 1)}R$$
$$+ \frac{G_p(1 - Q)}{1 + G_pC + Q(G_n^{-1}G_p - 1)}D \tag{16}$$
$$+ \frac{1 - Q}{1 + G_pC + Q(G_n^{-1}G_p - 1)}N$$

OEBDOBC approach

Figure 3 illustrates the original form of OEBDOBC.[12] Its equivalent block diagram can be obtained by replacing G_p, d pair with G_n, d_l pair, respectively. K_{obs} block requires an observer design. Let y_n denotes the nominal plant output and y_{obs} denotes the observer output.

The following equation can be written using the noiseless plant output in Figure 3 and OEBDOBC equivalent block diagram

$$(U + D)G_p = (U + D_l)G_n \tag{17}$$

As a consequence, the lumped disturbances are obtained as below

$$D_l = G_n^{-1}G_pD + (G_n^{-1}G_p - 1)U \tag{18}$$

From OEBDOBC equivalent block diagram, we have
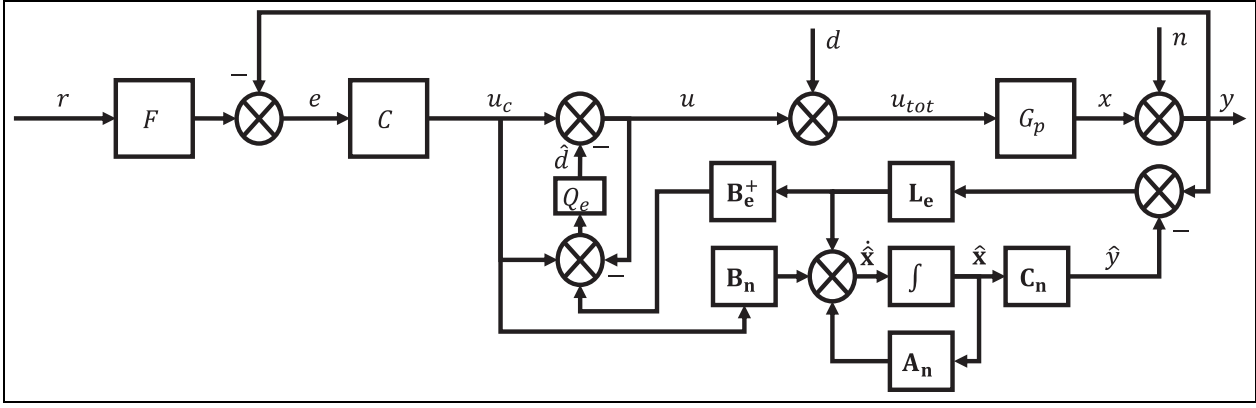
$$\hat{D} = Q_kG_nD_l + Q_kN \tag{19}$$

Figure 4. General block diagram of EID approach.

where Q_k is as follows

$$Q_k = \frac{K_{obs}}{1 + K_{obs}G_n} \tag{20}$$

From Figure 3, it can be seen that the OEBDOBC structure contains the CFC structure. The nine relations for the OEBDOBC system can be obtained as follows. From equations (2), (13) and (18)–(20), we have

$$
\begin{aligned}
U =\ & \frac{CF}{1 + G_pC + Q_kG_n(G_n^{-1}G_p - 1)}R \\
& - \frac{G_p(C + Q_k)}{1 + G_pC + Q_kG_n(G_n^{-1}G_p - 1)}D \\
& - \frac{C + Q_k}{1 + G_pC + Q_kG_n(G_n^{-1}G_p - 1)}N
\end{aligned}
\tag{21}
$$

From equations (4), (12) and (21), we have

$$
\begin{aligned}
X =\ & \frac{G_pCF}{1 + G_pC + Q_kG_n(G_n^{-1}G_p - 1)}R \\
& + \frac{G_p(1 - Q_kG_n)}{1 + G_pC + Q_kG_n(G_n^{-1}G_p - 1)}D \\
& - \frac{G_p(C + Q_k)}{1 + G_pC + Q_kG_n(G_n^{-1}G_p - 1)}N
\end{aligned}
\tag{22}
$$

From equations (5) and (22), we have

$$
\begin{aligned}
Y =\ & \frac{G_pCF}{1 + G_pC + Q_kG_n(G_n^{-1}G_p - 1)}R \\
& + \frac{G_p(1 - Q_kG_n)}{1 + G_pC + Q_kG_n(G_n^{-1}G_p - 1)}D \\
& + \frac{1 - Q_kG_n}{1 + G_pC + Q_kG_n(G_n^{-1}G_p - 1)}N
\end{aligned}
\tag{23}
$$

It can be seen that $Q = Q_kG_n$ from equations (21)–(23). If K_{obs} is chosen as given below, OEBDOBC and CDOBC approaches display identical performances

$$K_{obs} = \frac{Q}{G_n(1 - Q)} \tag{24}$$

EID approach

Figure 4 illustrates the original form of EID structure.[13,14] Its equivalent block diagram can be obtained by replacing G_p, d pair with G_n, d_l pair, respectively. In the figure, Q_e is the disturbance filter. In the diagram depicted in Figure 4, $\mathbf{A_n, B_n, C_n}$ are system matrix, control matrix and output matrix of nominal plant in controllable canonical form (CCF), respectively. $\mathbf{L_e}$ block is the observer gain. Furthermore, $\hat{\mathbf{x}}, \hat{y}$ denote the observer plant state and its output, respectively.

The following equation can be written using the noiseless plant output in Figure 4 and EID approach equivalent block diagram

$$(U + D)G_p = (U + D_l)G_n \tag{25}$$

As a consequence, the lumped disturbances are modeled by

$$D_l = G_n^{-1}G_pD + (G_n^{-1}G_p - 1)U \tag{26}$$

Performing the aforementioned substitutions, from the equivalent structure of the EID approach, we have

$$\hat{D} = k_1D_l + k_2U + k_3N \tag{27}$$

where $k_1 = \frac{(\mathbf{B_e^+ L_e} - b_e)G_nQ_e}{1 + (a_e - 1)Q_e}$, $k_2 = \frac{((\mathbf{B_e^+ L_e} - b_e)G_n - a_e)Q_e}{1 + (a_e - 1)Q_e}$, $k_3 = \frac{(\mathbf{B_e^+ L_e} - b_e)Q_e}{1 + (a_e - 1)Q_e}$, $k_1 = G_nk_3$, $k_2 = k_1 - \frac{a_eQ_e}{1 + (a_e - 1)Q_e}$, $a_e = (\mathbf{B_e^+ L_e})(\mathbf{C_n(HB_n)})$, $b_e = (\mathbf{B_e^+ L_e})(\mathbf{C_n(HL_e)})$, $\mathbf{H} = (s\mathbf{I} - \mathbf{A_n} + \mathbf{L_e C_n})^{-1}$ and $\mathbf{B_e^+} = (\mathbf{B_n}^T\mathbf{B_n})^{-1}(\mathbf{B_n}^T)$. ($\mathbf{A_n} \in \Re^{q \times q}$, $\mathbf{B_n} \in \Re^{q \times 1}$, $\mathbf{C_n} \in \Re^{1 \times q}$, $\mathbf{L_e} \in \Re^{q \times 1}$, $\mathbf{B_e^+} \in \Re^{1 \times q}$, $\hat{\mathbf{X}} \in \Re^{q \times 1}$, $\mathbf{H} \in \Re^{q \times q}$).
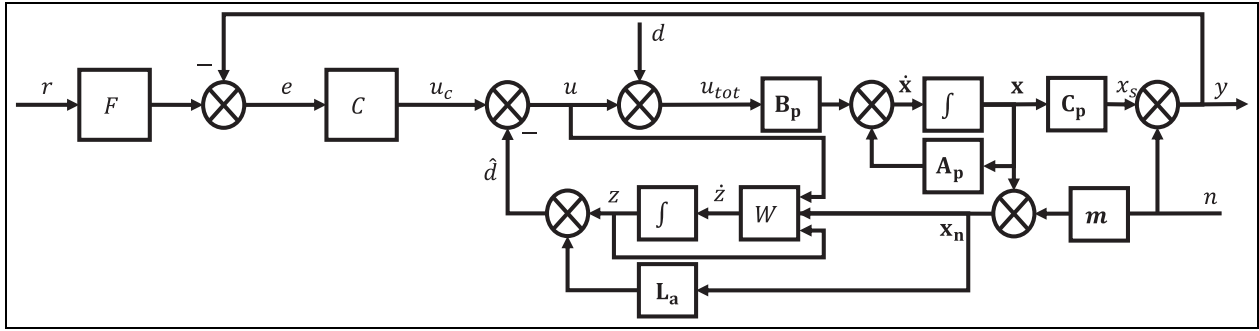
Figure 5. General block diagram of TDDOBC.

EID approach requires an observer design and a LPF (Q_e) design independently. From Figure 4, it can be seen that the EID structure contains the CFC structure too.

The nine relations for an EID system can be obtained as follows. From equations (2), (13), (26) and (27), we have

$$U = \frac{CF}{1 + G_pC + k_1(G_n^{-1}G_p - 1) + k_2}R$$
$$- \frac{G_p(C + k_1G_n^{-1})}{1 + G_pC + k_1(G_n^{-1}G_p - 1) + k_2}D \qquad (28)$$
$$- \frac{C + k_3}{1 + G_pC + k_1(G_n^{-1}G_p - 1) + k_2}N$$

From equations (4), (12) and (28), we have

$$X = \frac{G_pCF}{1 + G_pC + k_1(G_n^{-1}G_p - 1) + k_2}R$$
$$+ \frac{G_p(1 - k_1 + k_2)}{1 + G_pC + k_1(G_n^{-1}G_p - 1) + k_2}D \qquad (29)$$
$$- \frac{G_p(C + k_3)}{1 + G_pC + k_1(G_n^{-1}G_p - 1) + k_2}N$$

From equations (5) and (29), we have

$$Y = \frac{G_pCF}{1 + G_pC + k_1(G_n^{-1}G_p - 1) + k_2}R$$
$$+ \frac{G_p(1 - k_1 + k_2)}{1 + G_pC + k_1(G_n^{-1}G_p - 1) + k_2}D \qquad (30)$$
$$+ \frac{1 - k_1 + k_2}{1 + G_pC + k_1(G_n^{-1}G_p - 1) + k_2}N$$

TDDOBC approach

Figure 5 illustrates the original form of TDDOBC structure.[10] Its equivalent block diagram can be obtained by replacing $\mathbf{A_p}, \mathbf{B_p}, \mathbf{C_p}, d$ variables with $\mathbf{A_n}, \mathbf{B_n}, \mathbf{C_n}, d_l$, respectively. While $\mathbf{A_n}, \mathbf{B_n}, \mathbf{C_n}$ are system matrix, control matrix and output matrix of nominal plant in CCF, respectively, $\mathbf{A_p}, \mathbf{B_p}, \mathbf{C_p}$ are system matrix, control matrix and output matrix of disturbed uncertain plant in CCF, respectively. In the figure, $\mathbf{L_a}$ stands for the observer gain, $\mathbf{x}, \mathbf{x_n}, x_s$ denote the plant state, its noiseless output and its noisy output, respectively. The variable z in the figure denotes an auxiliary variable.

The following equality can be written using the noiseless plant output in Figure 5 and TDDOBC equivalent block diagram, which is obtained after the above stated substitutions

$$(U + D)G_p = (U + D_l)G_n \qquad (31)$$

As a consequence, the lumped disturbances are obtained as follows

$$D_l = G_n^{-1}G_pD + (G_n^{-1}G_p - 1)U \qquad (32)$$

From TDDOBC equivalent block diagram, we have

$$\hat{D} = z + \mathbf{L_a}\mathbf{x_n} \qquad (33)$$

The block labeled W in Figure 5 introduces the following dynamics

$$\dot{z} = -\mathbf{L_a}\mathbf{B_n}(z + \mathbf{L_a}\mathbf{x_n}) - \mathbf{L_a}(\mathbf{A_n}\mathbf{x_n} + \mathbf{B_n}u) \qquad (34)$$

From equations (33) and (34), we obtain

$$\hat{D} = (G_1 - G2)U + G_1D_l + G_3N \qquad (35)$$

where $\mathbf{a_t} = -(\mathbf{L_a}\mathbf{B_n})\mathbf{L_a} - \mathbf{L_a}\mathbf{A_n} + (s + \mathbf{L_a}\mathbf{B_n})\mathbf{L_a}$, $\mathbf{b_t} = (s\mathbf{I} - \mathbf{A_n})^{-1}\mathbf{B_n}$, $G_1 = \frac{\mathbf{a_t}\mathbf{b_t}}{s + \mathbf{L_a}\mathbf{B_n}}$, $G_2 = \frac{\mathbf{L_a}\mathbf{B_n}}{s + \mathbf{L_a}\mathbf{B_p}}$, $G_3 = \frac{\mathbf{a_t}\mathbf{m}}{s + \mathbf{L_a}\mathbf{B_n}}$, $\mathbf{m} = [1, \ldots, 1]^T$, ($\mathbf{a_t} \in \Re^{1 \times q}$, $\mathbf{b_t} \in \Re^{q \times 1}$, $\mathbf{L_a} \in \Re^{1 \times q}$, $\mathbf{x_n} \in \Re^{q \times 1}$, $\mathbf{A_n} \in \Re^{q \times q}$, $\mathbf{B_n} \in \Re^{q \times 1}$, $\mathbf{m} \in \Re^{q \times 1}$).

TDDOBC approach requires an observer design. From Figure 5, it can be seen that the TDDOBC structure contains the CFC structure. Therefore, the first five equations in CFC section can be used with the following corrections for the derivation of the nine TFs

$$X_s = G_pU_{tot} \qquad (36)$$

Figure 6. General block diagram of UDE approach.

$$Y = X_s + N \qquad (37)$$

From equations (2), (13), (32) and (35), we have

$$
\begin{aligned}
U = &\frac{CF}{1 + G_pC + G_1G_n^{-1}G_p - G_2}R \\
&- \frac{G_p(C + G_1G_n^{-1})}{1 + G_pC + G_1G_n^{-1}G_p - G_2}D \\
&- \frac{C + G_3}{1 + G_pC + G_1G_n^{-1}G_p - G_2}N
\end{aligned}
\qquad (38)
$$

From equations (12), (36) and (38), we have

$$
\begin{aligned}
X_s = &\frac{G_pCF}{1 + G_pC + G_1G_n^{-1}G_p - G_2}R \\
&+ \frac{G_p(1 - G_2)}{1 + G_pC + G_1G_n^{-1}G_p - G_2}D \\
&- \frac{G_p(C + G_3)}{1 + G_pC + G_1G_n^{-1}G_p - G_2}N
\end{aligned}
\qquad (39)
$$

From equations (37) and (39), we have

$$
\begin{aligned}
Y = &\frac{G_pCF}{1 + G_pC + G_1G_n^{-1}G_p - G_2}R \\
&+ \frac{G_p(1 - G_2)}{1 + G_pC + G_1G_n^{-1}G_p - G_2}D \\
&+ \frac{1 + G_p(G_1G_n^{-1} - G_3) - G_2}{1 + G_pC + G_1G_n^{-1}G_p - G_2}N
\end{aligned}
\qquad (40)
$$

UDE approach

Figure 6 illustrates the original form of the UDE approach.[16,17] UDE approach is based on a reference model, an error feedback gain and a LPF (G_f). Unlike other DOBC schemes, UDE structure does not contain the CFC structure. In Figure 6, $\mathbf{A_m}, \mathbf{B_m}$ are system matrix and control matrix of the reference plant model, respectively, $\mathbf{A_p}, \mathbf{B_p}, \mathbf{C_p}$ are system matrix, control matrix and output matrix of disturbed uncertain plant in observable canonical form (OCF), respectively. $\mathbf{A_n}$ is the system matrix of nominal plant in OCF. Besides, $\mathbf{K_m}$ is the feedback gain, $\mathbf{x_m}$ denotes the reference model plant state, $\mathbf{x}, \mathbf{x_s}, \mathbf{x_n}$ denote the disturbed uncertain plant state, its noiseless output and its noisy output, respectively.

The following equations can be obtained from Figure 6

$$\mathbf{X_m} = (s\mathbf{I} - \mathbf{A_m})^{-1}\mathbf{B_m}FR \qquad (41)$$

Control signal U is as follows

$$
\begin{aligned}
U = &G_1(\mathbf{B_u^+}((s\mathbf{I})\mathbf{X_m})) \\
&- G_1(\mathbf{B_u^+}(\mathbf{V_m}(\mathbf{X_m} - \mathbf{X_n}))) \\
&- \mathbf{B_u^+}\mathbf{A_n}\mathbf{X_n} - G_2\mathbf{B_u^+}\mathbf{X_n}
\end{aligned}
\qquad (42)
$$

$$\mathbf{X_n} = \mathbf{X} + \mathbf{m}N \qquad (43)$$

$$\mathbf{X} = (s\mathbf{I} - \mathbf{A_p})^{-1}\mathbf{B_p}(U + D) \qquad (44)$$

$$X_s = \mathbf{C_p}\mathbf{X} \qquad (45)$$

Table 1. GoF equations(* Irrelevant inputs are taken as zero).

Strategy	CSF *	SF *	DSF *	NSF *
CFC	U_c/D or X/N	Y/N	X/D	U_c/N
CDOBC	U/D or X/N	Y/N	X/D	U/N
OEBDOBC	U/D or X/N	Y/N	X/D	U/N
EID	U/D or X/N	Y/N	X/D	U/N
TDDOBC	U/D or X_s/N	$(I - U/D)$ or $(I - X_s/N)$	X_s/D	U/N
UDE	U/D or X_s/N	$(I - U/D)$ or $(I - X_s/N)$	X_s/D	U/N

CSF: complementary sensitivity function; DSF: disturbance sensitivity function; NSF: noise sensitivity function; CFC: classical feedback control; CDOBC: conventional disturbance observer based control; OEBDOBC: output error-based disturbance observer based control; EID: equivalent input disturbance; TDDOBC: time domain disturbance observer based control; UDE: uncertainty disturbance estimator.

$$Y = X_s + N \tag{46}$$

where $G_1 = \frac{1}{1-G_f}$, $G_2 = \frac{sG_f}{1-G_f}$, $\mathbf{V_m} = (\mathbf{A_m} + \mathbf{K_m})$, $\mathbf{B_u}^+ = (\mathbf{B_n}^T\mathbf{B_n})^{-1}\mathbf{B_n}^T$, $\mathbf{m} = [1, \dots, 1]^T$, $(\mathbf{X_m} \in \Re^{q \times 1}$, $\mathbf{X_n} \in \Re^{q \times 1}$, $\mathbf{X} \in \Re^{q \times 1}$, $\mathbf{A_*} \in \Re^{q \times q}$, $\mathbf{B_*} \in \Re^{q \times 1}$, $\mathbf{C_*} \in \Re^{1 \times q}$, $\mathbf{V_m} \in \Re^{q \times q}$, $\mathbf{K_m} \in \Re^{q \times q}$, $\mathbf{B_u}^+ \in \Re^{1 \times q}$, $\mathbf{m} \in \Re^{q \times 1})$.

The nine relations for an UDE system can be obtained as follows. From equations (41)–(44), we have

$$U = \frac{a_u F}{1 - \mathbf{b_u}((s\mathbf{I} - \mathbf{A_p})^{-1}\mathbf{B_p})} R$$
$$- \frac{-\mathbf{b_u}((s\mathbf{I} - \mathbf{A_p})^{-1}\mathbf{B_p})}{1 - \mathbf{b_u}((s\mathbf{I} - \mathbf{A_p})^{-1}\mathbf{B_p})} D \tag{47}$$
$$- \frac{-\mathbf{b_u m}}{1 - \mathbf{b_u}((s\mathbf{I} - \mathbf{A_p})^{-1}\mathbf{B_p})} N$$

where $a_u = G_1(\mathbf{B_u}^+((s\mathbf{I} - \mathbf{V_m})((s\mathbf{I} - \mathbf{A_m})^{-1}\mathbf{B_m})))$ and $\mathbf{b_u} = G_1(\mathbf{B_u}^+ \mathbf{V_m}) - \mathbf{B_u}^+ \mathbf{A_n} - G_2\mathbf{B_u}^+$, $(\mathbf{b_u} \in \Re^{1 \times q})$. From equations (44), (45) and (47), we have

$$X_s = \frac{\mathbf{C_p}(((s\mathbf{I} - \mathbf{A_p})^{-1}\mathbf{B_p})a_u F)}{1 - \mathbf{b_u}((s\mathbf{I} - \mathbf{A_p})^{-1}\mathbf{B_p})} R$$
$$+ \frac{\mathbf{C_p}((s\mathbf{I} - \mathbf{A_p})^{-1}\mathbf{B_p}))}{1 - \mathbf{b_u}((s\mathbf{I} - \mathbf{A_p})^{-1}\mathbf{B_p})} D \tag{48}$$
$$- \frac{-\mathbf{C_p}(((s\mathbf{I} - \mathbf{A_p})^{-1}\mathbf{B_p})(\mathbf{b_u m}))}{1 - \mathbf{b_u}((s\mathbf{I} - \mathbf{A_p})^{-1}\mathbf{B_p})} N$$

From equations (46) and (48), we have

$$Y = \frac{\mathbf{C_p}(((s\mathbf{I} - \mathbf{A_p})^{-1}\mathbf{B_p})a_u F)}{1 - \mathbf{b_u}((s\mathbf{I} - \mathbf{A_p})^{-1}\mathbf{B_p})} R$$
$$+ \frac{\mathbf{C_p}((s\mathbf{I} - \mathbf{A_p})^{-1}\mathbf{B_p}))}{1 - \mathbf{b_u}((s\mathbf{I} - \mathbf{A_p})^{-1}\mathbf{B_p})} D \tag{49}$$
$$+ \frac{P + 1 - \mathbf{b_u}((s\mathbf{I} - \mathbf{A_p})^{-1}\mathbf{B_p})}{1 - \mathbf{b_u}((s\mathbf{I} - \mathbf{A_p})^{-1}\mathbf{B_p})} N$$

where $P = \mathbf{C_p}(((s\mathbf{I} - \mathbf{A_p})^{-1}\mathbf{B_p})(\mathbf{b_u m}))$.

The gang of four equations

In the previous subsections, nine TFs of the five DOBC approaches are derived. These nine TFs provide useful insights for understanding and analyzing control systems employing disturbance observer sub-dynamics. They can be reduced to six equations because some of them are the same under certain rules (e.g. $F = 1$). In this article, the only GoF equations are considered as performance and robustness equations, and they are shown in Table 1 as a relationship TFs described in the previous subsections.

Simulation results

This section presents a robustness and performance analysis approach using GoF equations for five DOBC schemes. DOBC structures generally require a LPF design as described in the previous sections. LPF characteristics are important as they directly affect the disturbance rejection performance of DOBC approaches. If the LPF bandwidth is chosen too high, the robustness and stability of the system are adversely affected.[21] Therefore, the choice of LPF order and its bandwidth is critical. In this article, the following first order LPF is selected for all DOBC approaches to be able to compare all DOBC approaches under the same conditions. The bandwidth of the LPF is chosen wide enough for all simulation studies. One could choose higher order LPF structures, but this would increase the computational burden of the design

$$LPF(s) = \frac{T}{s + T} \tag{50}$$

where T is the cutoff frequency of the LPF.

Simulation parameters

It should be noted that as this study gives a comprehensive comparison of disturbance observer based robust control approaches, structural details and complexity of each approach, instead of a particular plant model with its own challenges, a second order plant model with some uncertainty in the form of time delay is

Table 2. Controller design performance criteria.

Rising time (s)	Settling time (s)	Max. overshoot
< 0.3	< 0.8	< %5

considered. Although the studied plant model is an abstract one, this makes it possible to compare the most critical aspects aside from the plant-specific difficulties.

Minimum-phase uncertain plant. Nominal plant and the uncertain plant considered in this part are as follows[22]

$$G_n(s) = \frac{s+5}{s^2 + 5s + 6}, G_p(s) = G_n(s)(1 + \Delta W_T(s)) \tag{51}$$

where $\Delta = 0.3$ and uncertainty weighting function is $W_T(s) = (5s + 100)/(s + 500)$.

Minimum-phase uncertain plant with time delay. Nominal plant and uncertain plant with time delay for this part are considered as follows[22]

$$G_p(s) = G_n(s)(1 + \Delta W_T(s))e^{-\tau s} \tag{52}$$

where $\Delta = 0.3$, $W_T(s) = (5s + 100)/(s + 500)$ and the time delay $\tau = 0.01s$.

CFC parameters. It is well known that cancelation of slow or unstable poles by zeros adversely affects the disturbance rejection performance of a controller. Therefore, classical feedback controller equation (53) is designed using pole placement method with the specifications given in Table 2. At the same time, for UDE approach, reference model meeting the criteria in Table 2 is selected as given in equation (54)

$$C(s) = \frac{6.75(s + 12.25s + 18)}{s + 12.25s} \tag{53}$$

$$\mathbf{A_m} = \begin{bmatrix} -5 & -6.25 \\ 1 & 0 \end{bmatrix}, \mathbf{B_m} = \begin{bmatrix} 6.25 \\ 0 \end{bmatrix}, \mathbf{C_m} = \begin{bmatrix} 0 & 1 \end{bmatrix} \tag{54}$$

CDOBC parameters. $Q(s)$ filter is selected as follows

$$Q(s) = \frac{100}{s + 100} \tag{55}$$

OEBDOBC parameters. Together with the Q in equation (55), $K_{obs}(s)$ is selected as follows

$$K_{obs}(s) = \frac{Q(s)}{G_n(s)(1 - Q(s))} \tag{56}$$

EID parameters. $Q_e(s)$ filter is selected as follows

$$Q_e(s) = \frac{100}{s + 100} \tag{57}$$

$\mathbf{L_e}$ is designed using Ackermann's formula as follows

$$\mathbf{L_e} = \begin{bmatrix} 20 \\ 1 \end{bmatrix} \tag{58}$$

TDDOBC parameters. $\mathbf{L_a}$ is designed using Ackermann's formula as follows

$$\mathbf{L_a} = \begin{bmatrix} 112.66 \\ -17.33 \end{bmatrix} \tag{59}$$

UDE parameters. $G_f(s)$ filter is selected as follows

$$G_f(s) = \frac{100}{s + 100} \tag{60}$$

Performance and robustness discussion

Order of the LPF and its bandwidth directly affect the disturbance rejection capability of a DOBC scheme. For all DOBC approaches presented in this article, a first order LPF for relevant approaches is used, and bandwidths of them are set to 100 rad/s. While Figures 7–10 show the response of GoF for uncertain minimum phase plant without time delay, Figures 11–14 illustrate the results for uncertain minimum phase plant containing time delay.

In Figure 7, we illustrate the step responses of the DSF given in equation (51). Because of our identical LPF selections and the choice in equation (56), spectral views of the GoF TFs are identical for CDOBC and OEBDOBC. Clearly, CFC in this figure displays the poorest performance. According to the figure, all schemes produce acceptable results. Their disturbance suppression capability ranking from best to worst is as follows: TDDOBC, CDOBC-OEBDOBC, UDE, EID and CFC. In this sorting, we consider the peak magnitude and the convergence speed as the major metrics.

Figure 8 depicts the NSF behaviors. Looking at the results, we see some approaches produce higher sensitivity at low frequencies and some in high frequencies. Assuming the disturbances are low frequency inputs and the chosen Q filters have a bandwidth of 100 rad/s, the poorest performance in this picture is obtained with UDE approach because of the ≈ 15 dB gain in the low frequency region. Other approaches have a small sensitivity in the low frequencies, yet the sensitivity curves increase as the frequency increases. Interestingly, EID approach displays a peak around 50 rad/s and the curve falls as the frequency approaches 100 rad/s and the insensitivity to noise is recovered for high frequencies.
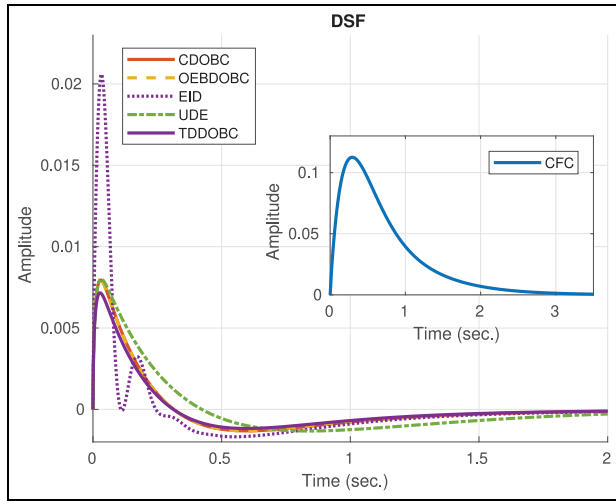
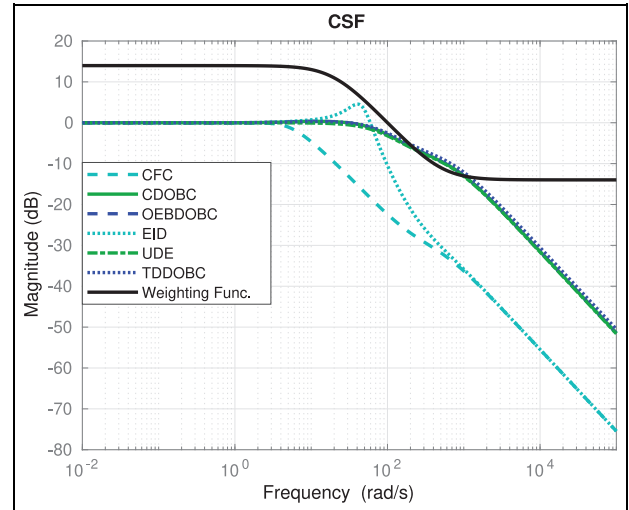**Figure 7.** Step response of the disturbance sensitivity function without time delay.

Figure 9. Frequency response of the complementary sensitivity function without time delay.
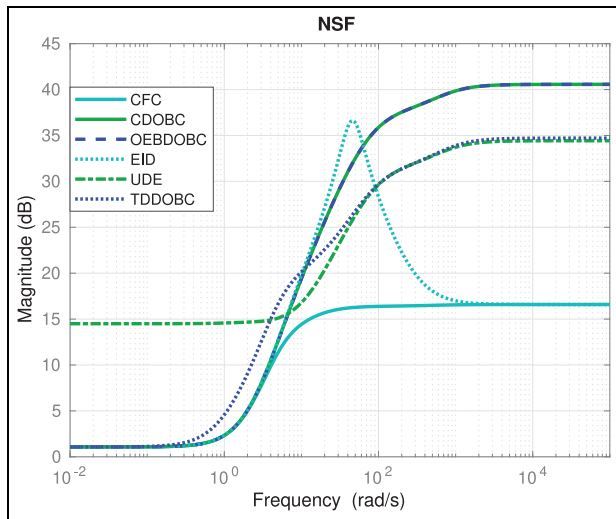

Figure 8. Frequency response of the noise sensitivity function without time delay.
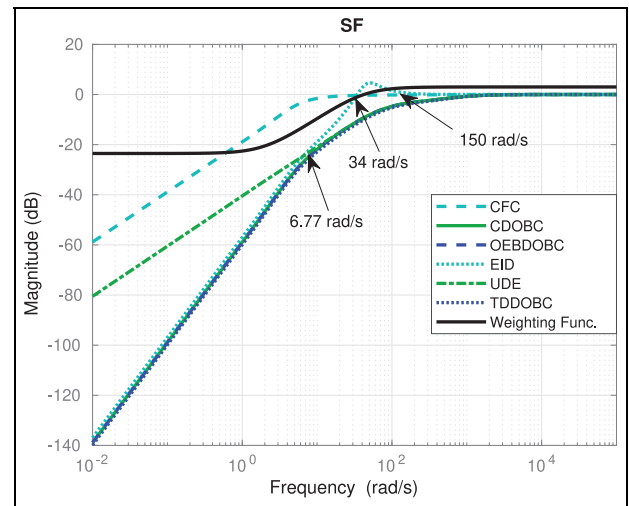

Figure 10. Frequency response of the sensitivity function frequency response without time delay.

In terms of noise input, we desire smaller magnitudes in high frequencies, and this is obtained best with CFC approach. The level of insensitivity to noise from the highest to lowest: CFC, EID, TDDOBC, CDOBC-OEBDOBC and UDE.

In Figure 9, we show the frequency responses of the CSFs for each approach. In this figure, we see that EID approach is poorer than the other DOBC schemes, which maintain the 0 dB level over a fairly large bandwidth without displaying any resonant peaks. EID approach is more vulnerable to waterbed effect, which shows itself as a peak provoked in between 6.77 and 59 rad/s, than its alternatives. We sort the approaches according to the bandwidth, and from the largest to the smallest bandwidth are TDDOBC, CDOBC-OEBDOBC, UDE, EID and CFC. CSF figure recommends the TDDOBC as it displays the highest bandwidth.

Figure 10 presents the frequency responses of the SFs. In the figure, all DOBC schemes fairly suppress the components below 6.77 rad/s. The suppression capability in the low frequency region sorted from the strongest to the weakest is TDDOBC, CDOBC-OEBDOBC, UDE, EID and CFC. EID approach has a weaker disturbance attenuation performance for the components between 6.77 and 34 rad/s than the other schemes. In addition, EID approach amplifies the components between 34 and 150 rad/s, which is a negative observation. For high frequencies, all approaches feature high pass filters. In producing these results, the weighting performance function of SF is selected as $W_S(s) = (0.707s + 30)/(s + 2)$.

In the next GoF plots, we will consider the time delay effect in the overall performance. Figure 11 illustrates the step responses of the DSF given in equation (52). The worst disturbance rejection performance among the
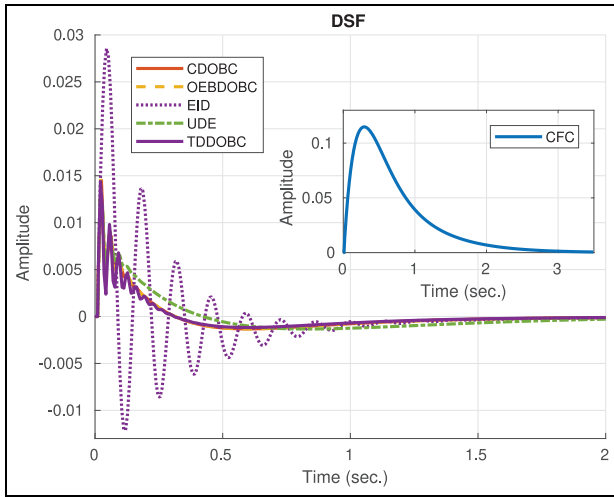
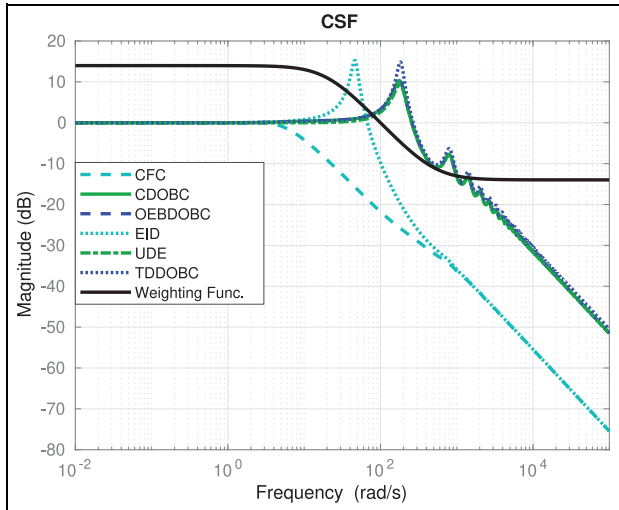**Figure 11.** Step response of the disturbance sensitivity function with time delay.

Figure 12. Frequency response of the noise sensitivity function with time delay.

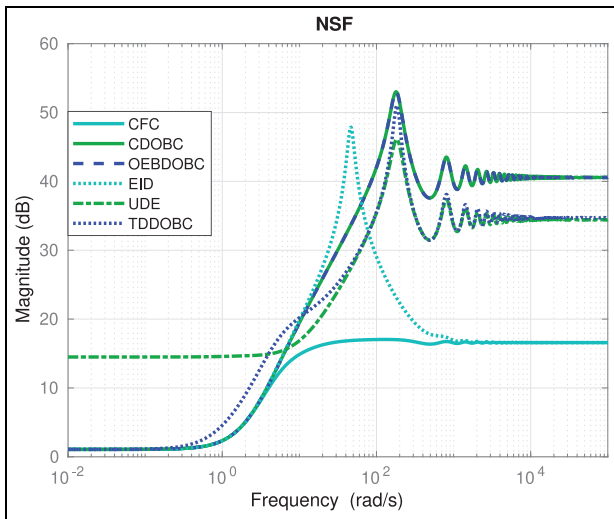**Figure 13.** Frequency response of the complementary sensitivity function with time delay.
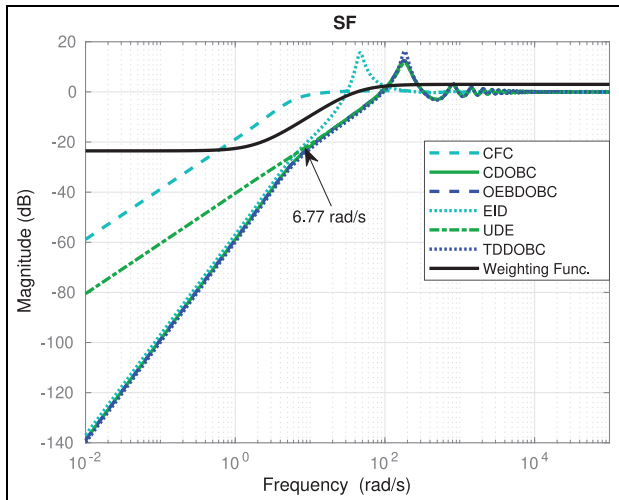

Figure 14. Frequency response of the sensitivity function with time delay.

studied approaches is CFC approach, which is shown separately in the window plot. As can be seen from Figure 11, disturbance rejection performances can be sorted from the best to worst as CDOBC-OEBDOBC, UDE, TDDOBC, EID and CFC. Time delay increases the oscillations in the step responses for almost all DOBC schemes. However, the figure shows that it severely affects EID and TDDOBC approaches, the responses of which display an oscillatory initial transient.

Figure 12 shows frequency responses of the NSF under time delay conditions. We see that the time delay increases the sensitivity to noise for all DOBC approaches in high frequencies except CFC approach. The noise sensitivity responses from the strongest to weakest can be sorted as CFC (most insensitive to noise), EID, TDDOBC, CDOBC-OEBDOBC and UDE (most sensitive to noise).

In Figure 13, we present the CSF behaviors under time delay conditions. Time delay makes the EID

approach more vulnerable to waterbed effect than other approaches. This is visible from the peak observed between 5 and 67 rad/s. Yet, EID recovers for high frequencies with a poor bandwidth. In this figure, CFC displays the poorest performance then comes the EID approach. This is mainly because of the bandwidth comparison with the other approaches, which display a resonant peak around 190 rad/s and the ordering is done by considering the magnitude at this frequency. This leads to the following sorting UDE, CDOBC-OEBDOBC, TDDOBC, EID and CFC.

Figure 14 depicts frequency responses of the SF under time delay conditions. When Figure 14 is examined, it can be seen that the time delay increases the amplification magnitude of EID approach between 31 and 150 rad/s. The other approaches try to preserve the high pass filter properties with some oscillations after 100 rad/s. As discussed for Figure 10, the attenuation

Table 3. Fundamental properties of the approaches.

	CDOBC	OEBDOBC	EID	TDDOBC	UDE
Inverse required	Yes	No	No	No	No
Waterbed effect vulnerability	No	No	Yes	No	No
Insensitivity to measurement noise	Poor	Poor	Good	Poor	Very poor
Insensitivity to time delay	Good	Good	Very poor	Poor	Very good
Structure	TF	TF	TF-CCF	CCF	OCF

CDOBC: conventional disturbance observer based control; OEBDOBC: output error-based disturbance observer based control; EID: equivalent input disturbance; TDDOBC: time domain disturbance observer based control; UDE: uncertainty disturbance estimator; TF: transfer function; TF-CCF: transfer function-controllable canonical form; OCF: observable canonical form.

Table 4. DOBC performance rankings for the measures DSF, NSF, CSF and SF (* denotes time delay).

	1	2	3	4	5
DSF	TDDOBC	CDOBC-OEBDOBC	UDE	EID	CFC
NSF	CFC	EID	TDDOBC	CDOBC-OEBDOBC	UDE
CSF	TDDOBC	CDOBC-OEBDOBC	UDE	EID	CFC
SF	TDDOBC	CDOBC-OEBDOBC	UDE	EID	CFC
DSF *	CDOBC-OEBDOBC	UDE	TDDOBC	EID	CFC
NSF *	CFC	EID	TDDOBC	CDOBC-OEBDOBC	UDE
CSF *	UDE	CDOBC-OEBDOBC	TDDOBC	EID	CFC
SF *	TDDOBC	CDOBC-OEBDOBC	UDE	EID	CFC

DSF: disturbance sensitivity function; TDDOBC: time domain disturbance observer based control; CDOBC-OEBDOBC: conventional disturbance observer based control–output error-based disturbance observer based control; UDE: uncertainty disturbance estimator; EID: equivalent input disturbance; CFC: classical feedback control; NSF: noise sensitivity function; CSF: complementary sensitivity function.

capability order for the low frequency components from strongest to weakest is TDDOBC, CDOBC-OEBDOBC, UDE, EID and CFC. EID approach has a better suppression performance than UDE approach below 6.77 rad/s. Considering the resonant peak magnitude around 190 rad/s, UDE approach produces the smallest peak magnitude, which is a good property.

As discussed above, OEBDOBC approach produces identical results with CDOBC approach since K_{obs} is chosen as in equation (56). Although they have the same performance, OEBDOBC proposed in Kürkçü et al.[23] does not require the inverse of nominal plant model and it is advisable also for non-minimum phase systems when compared to CDOBC structure.

Table 3 gives a summary of fundamental properties of the approaches, namely the necessity to an inverse nominal model, vulnerability to waterbed effect, insensitivity to noise and time delays, and the structural representation are listed for each approach.

Table 4 lists the rankings given above for the practicing engineers, who may give more importance to one quality than the others. In the table, Column 1 represents the well performing approach(es), whereas the Column 5 gives the poor performing one(s). According to the table, if there is no time delay in the process model, TDDOBC is a satisfactorily successful approach with average performance in NSF measure. Under time delay conditions, TDDOBC provides average performance, yet, we see that the CDOBC-OEBDOBC

approaches perform well in general. The table does not recommend a particular approach persistently, and the contribution of this work is to unfold the approaches, which perform well and poor for which of the measures named DSF, NSF, CSF and SF.

Conclusion

This article comparatively discusses five DOBC approaches, namely CDOBC, OEBDOBC, EID, TDDOBC, UDE. Their common and equivalent block diagram properties have been discussed, and nine performance and robustness TFs that provide an in-depth understanding of these schemes are derived. Four of these TFs are selected as a GoF equations, and for both uncertain minimum phase and time delay system, robustness and disturbance rejection performance discussion have been given for five DOBC schemes and CFC scheme. Our tests have shown that derived GoF equations can be used for qualifying the DOBC performances. A summary table considering performance and robustness analysis of DOBC methods and their design requirements are presented. In terms of robustness and disturbance rejection performance under similar operating conditions, simulation results recommend the TDDOBC scheme, which outperforms the other DOBC approaches if there is no process time delay. Under the time delay conditions, UDE approach is more advisable than the others.

ORCID iD

Abdurrahman Bayrak   https://orcid.org/0000-0001-6166-7894

References

1. Chen WH, Yang J, Guo L, et al. Disturbance-observer-based control and related methods—an overview. *IEEE Trans Ind Electron* 2016; 63(2): 1083–1095.
2. Ohishi K, Ohnishi K and Miyachi K. Torque-speed regulation of DC motor based on load torque estimation method. In: *Proceedings of the IEEJ international power electronics conference (IPEC-TOKYO)*, Tokyo, Japan, 1 December 1983, vol. 2, pp.1209–1216. Tokyo, Japan: The Institute of Electrical Engineers of Japan.
3. Ohishi K, Nakao M, Ohnishi K, et al. Microprocessor-controlled DC motor for load-insensitive position servo system. *IEEE Trans Ind Electron* 1987; IE-34(1): 44–49.
4. Nakao M, Ohnishi K and Miyachi K. A robust decentralized joint control based on interference estimation. In: *Proceedings of the IEEE international conference on robotics and automation*, Raleigh, NC, 31 March–3 April 1987, vol. 4, pp.326–331. New York: IEEE.
5. Han J. The "extended state observer" of a class of uncertain systems. *Control Decis* 1995; 10(1): 85–88.
6. Han J. From PID to active disturbance rejection control. *IEEE Trans Ind Electron* 2009; 56(3): 900–906.
7. Chang H, Kim H, Park G, et al. DO-DAT: a MATLAB toolbox for design & analysis of disturbance observer. *IFAC-PapersOnLine* 2018; 51(25): 340–345.
8. Uzunovic T, Sariyildiz E and Sabanovic A. A discussion on discrete implementation of disturbance-observer-based control. In: *Proceedings of the IEEE 15th international workshop on advanced motion control (AMC)*, Tokyo, Japan, 9–11 March 2018, pp.613–618. New York: IEEE.
9. Efe MÖ and Kasnakoğlu C. An enhanced bandwidth disturbance observer based control- S-filter approach. *Turk J Electr Eng Comput Sci*. Epub ahead of print 16 February 2021. DOI: 10.3906/elk-2009-13.
10. Yang J, Chen WH and Li S. Autopilot design of bank-to-turn missiles using state-space disturbance observers. In: *Proceedings of the UKACC international conference on control*, Coventry, 7–10 September 2010, pp.1–6. New York: IEEE.
11. Lazim IM, Husain AR, Mohamed Z, et al. Disturbance observer-based formation tracking control of multiple quadrotors in the presence of disturbances. *Trans Inst Meas Control* 2019; 41(14): 4129–4141.
12. Kürkçü B, Kasnakoğlu C and Efe MÖ. Disturbance/uncertainty estimator based integral sliding-mode control. *IEEE Trans Autom Control* 2018; 63(11): 3940–3947.
13. She JH, Fang M, Ohyama Y, et al. Improving disturbance-rejection performance based on an equivalent-input-disturbance approach. *IEEE Trans Ind Electron* 2008; 55(1): 380–389.
14. She JH, Xin X and Pan Y. Equivalent-input-disturbance approach—analysis and application to disturbance rejection in dual-stage feed drive control system. *IEEE/ASME Trans Mechatron* 2010; 16(2): 330–340.
15. Du Y, Cao W, She J, et al. Disturbance rejection and control system design using improved equivalent input disturbance approach. *IEEE Trans Ind Electron* 2019; 67(4): 3013–3023.
16. Zhong QC and Rees D. Control of uncertain LTI systems based on an uncertainty and disturbance estimator. *J Dyn Sys Meas Control* 2004; 126(4): 905–910.
17. Zhong QC, Kuperman A and Stobart RK. Design of UDE-based controllers from their two-degree-of-freedom nature. *Int J Rob Nonlin Control* 2011; 21(17): 1994–2008.
18. Aharon I, Shmilovitz D and Kuperman A. Phase margin oriented design and analysis of UDE-based controllers under actuator constraints. *IEEE Trans Ind Electron* 2018; 65(10): 8133–8141.
19. Li S, Yang J, Chen WH, et al. *Disturbance observer-based control: methods and applications*. Boca Raton, FL: CRC Press, 2014.
20. Sariyildiz E, Oboe R and Ohnishi K. Disturbance observer-based robust control and its applications: 35th anniversary overview. *IEEE Trans Ind Electron* 2019; 67(3): 2042–2053.
21. Sariyildiz E and Ohnishi K. Analysis the robustness of control systems based on disturbance observer. *Int J Control* 2013; 86(10): 1733–1743.
22. Sariyildiz E and Ohnishi K. A guide to design disturbance observer. *J Dyn Sys Meas Control* 2014; 136(2): 021011.
23. Kürkçü B, Kasnakoğlu C and Efe MÖ. Disturbance/uncertainty estimator based robust control of nonminimum phase systems. *IEEE/ASME Trans Mechatron* 2018; 23(4): 1941–1951.